

## **SUPPLEMENTAL MATERIAL**

### **COMPLETE METHODS**

#### **Animals**

Mice were maintained on a 12-h light/dark cycle and were given access to a standard laboratory diet and water ad libitum. To evaluate the effects of diabetic therapy on the changes in DNA methylation, we administered pioglitazone (Takeda Pharmaceutical, Osaka, Japan), a peroxisome proliferator-activated receptor- $\gamma$  agonist, to 5-week-old *db/db* mice for 3 weeks. Pioglitazone was mixed with normal mouse chow and administered at the dose of 15 mg/kg body wt/day, because 15 mg/kg of pioglitazone has been reported to attenuate albuminuria and changes of glomerular gene expression.<sup>1</sup>

Mice were killed under anesthesia with pentobarbital. Blood glucose levels were determined with G-checker, a compact glucose analyzer (GUNZE, Tokyo, Japan).

Triglyceride and non-esterified fatty acids were measured using L-type Wako TG-H kit (Wako Pure Chemical Industries, Tokyo, Japan) and NEFA SS kit (Eiken Co. Ltd., Tochigi, Japan), respectively. The urinary albumin concentration was measured using the mouse ELISA kit (Shibayagi, Gunma, Japan).

#### **Cell Culture**

To determine the effect of decreased DNA methylation on gene expression, HRPTEC

were treated with 100 nM 5-Aza-2'-deoxycytidine for 96 hours and harvested. For evaluation of the effects of HDAC inhibition, HRPTEC were incubated with TSA (300 nM) for 24 hours and harvested. For the combination of DNA demethylation and HDAC inhibition, cells were incubated with 100 nM 5-Aza-2'-deoxycytidine for 96 hours in combination with 300 nM TSA for the last 24 hours.

### **Sorting of the PT Cells**

The whole kidneys were cut into 5-mm<sup>3</sup> pieces with tweezers and scalpel in a Petri dish on ice. The pieces were loaded into a Medicone chamber (CTSV, Turin, Italy), and disaggregated into single cells by microblades spinning at a constant rate of 100 rpm. Cells were stained with fluorescein isothiocyanate-conjugated Lotus tetragonolobus lectin (Vector Laboratories, Burlingame, CA) as the marker of PT.<sup>2,3</sup> DNA and total RNA were extracted with AllPrep DNA/RNA Mini (QIAGEN K.K., Tokyo, Japan).

### **Genome-wide DNA Methylation Analysis**

In the D-REAM assay, DNA methylation status at HpyCH4IV sites were indicated by hybridization signals of GeneChip Mouse Promoter 1.0R Array (Affymetrix) with probes mapped to the 8.5-kb regions around transcription start sites of the RefSeq genes in the mouse genome (Build 37.1). Microarray signals were processed by MAT,<sup>4</sup> and converted to D-REAM scores of fragments digested in silico by HpyCH4IV. The

microarray data of the PT cells isolated in duplicate can be found at Array Express ([www.ebi.ac.uk/arrayexpress/](http://www.ebi.ac.uk/arrayexpress/), accession number E-MTAB-2620). By comparing the data of the PT cells (*db/m*) data with those of the liver, cerebrum, and kidney of C57BL/6J mice,<sup>5, 6</sup> we selected DMRs from HpyCH4IV sites that exhibited significantly different D-REAM scores at cut-off p-value of  $10^{-5}$ . The genes neighboring the DMRs were identified using the Galaxy web server.<sup>7, 8</sup> The gene ontology analysis was carried out using the DAVID web server.<sup>9</sup>

### **Combined bisulfite restriction analysis (COBRA) and bisulfite sequencing**

Bisulfite conversion of 150-500 ng genomic DNA was performed with the EZ DNA Methylation Kit (Zymo Research, Irvine, CA). The DNA fragments containing the DMRs were amplified by PCR. PCR was performed using Immolase DNA Polymerase (Bioline, London, UK) under the following conditions: 95 °C for 7 min; 43 cycles at 94 °C for 1 min, 55 °C or 50°C for 30 s, and 72 °C for 1 min; the final extension step at 72 °C for 10 min. For quantitative-COBRA, the PCR products were digested with HpyCH4IV, a methylation-sensitive restriction enzyme. After purification by gel filtration with Sephadex G-50 (GE Healthcare Life Sciences, Buckinghamshire, UK), the purified PCR products were analyzed with MutiNA, a microchip electrophoresis system (Shimadzu, Kyoto, Japan) and the methylation levels were quantified. For

bisulfite sequencing of the Agt promoter, PCR products were cloned into the pGEM-T Easy vector (Promega, Madison, WI, USA), and at least 20 clones were chosen randomly from each sample and sequenced. Methylation sites were visualized by the web-based tool, "QUMA" (<http://quma.cdb.riken.jp/>).

### **Quantitative RT-PCR analysis**

For quantitative RT-PCR analysis, the cDNA product was generated using a high-capacity cDNA archive kit (Applied Biosystems). The expression levels of Agt (mouse), AGT (human),  $\beta$ -actin, GAPDH, and Abcc4 were then analyzed using the TaqMan Universal PCR Master Mix (Applied Biosystems). For detection of other genes, SYBR Green PCR Master Mix (Applied Biosystems) was used. The primers and probes of Agt (mouse), AGT (human),  $\beta$ -actin, GAPDH, Abcc4, and 18S ribosomal RNA were obtained from Applied Biosystems. Expression levels were normalized to those of 18S ribosomal RNA for experiments using the whole kidney and those of  $\beta$ -actin for other experiments with mice. GAPDH was used for normalization in experiments with HRPTEC.

### **In Situ Hybridization**

Kidneys were fixed with Tissue Fixative (GenoStaff, Inc., Tokyo, Japan), then embedded in paraffin and sectioned at 6  $\mu$ m. In situ hybridization was performed

according to a previously described method.<sup>10</sup> For generation of antisense and sense cRNA probes, a 541-bp DNA fragment corresponding to the nucleotide positions 5–545 of the mouse gene for *Agt* (GenBank accession number NM\_007428) was used. Sense probes were used as hybridization control. The bound label was detected using NBT-BCIP solution (Sigma), an alkaline phosphate color substrate.

### **ChIP Assay**

Frozen kidneys were pulverized by mortar and pestle to a powder before fixation with 10% formaldehyde. ChIP assay was performed in the kidney or HRPTEC as described previously.<sup>11</sup> Immunoprecipitated DNA was quantified by quantitative-real time PCR using SYBR Green PCR Master Mix. The enrichment of DNA in the immunoprecipitates was calculated relative to the input samples.

### **REFERENCES**

1. Makino H, Miyamoto Y, Sawai K, Mori K, Mukoyama M, Nakao K, Yoshimasa Y, Suga S: Altered gene expression related to glomerulogenesis and podocyte structure in early diabetic nephropathy of db/db mice and its restoration by pioglitazone. *Diabetes* 55: 2747-2756, 2006
2. Cachat F, Lange-Sperandio B, Chang AY, Kiley SC, Thornhill BA, Forbes MS,

- Chevalier RL: Ureteral obstruction in neonatal mice elicits segment-specific tubular cell responses leading to nephron loss. *Kidney Int* 63: 564-575, 2003
3. Hiesberger T, Bai Y, Shao X, McNally BT, Sinclair AM, Tian X, Somlo S, Igarashi P: Mutation of hepatocyte nuclear factor-1beta inhibits Pkhd1 gene expression and produces renal cysts in mice. *J Clin Invest* 113: 814-825, 2004
  4. Johnson WE, Li W, Meyer CA, Gottardo R, Carroll JS, Brown M, Liu XS: Model-based analysis of tiling-arrays for ChIP-chip. *Proc Natl Acad Sci U S A* 103: 12457-12462, 2006
  5. Kikuchi R, Yagi S, Kusuhara H, Imai S, Sugiyama Y, Shiota K: Genome-wide analysis of epigenetic signatures for kidney-specific transporters. *Kidney Int* 78: 569-577, 2010
  6. Yagi S, Hirabayashi K, Sato S, Li W, Takahashi Y, Hirakawa T, Wu G, Hattori N, Ohgane J, Tanaka S, Liu XS, Shiota K: DNA methylation profile of tissue-dependent and differentially methylated regions (T-DMRs) in mouse promoter regions demonstrating tissue-specific gene expression. *Genome Res* 18: 1969-1978, 2008
  7. Goecks J, Nekrutenko A, Taylor J: Galaxy: a comprehensive approach for supporting accessible, reproducible, and transparent computational research in the

- life sciences. *Genome Biol* 11: R86, 2010
8. Karolchik D, Hinrichs AS, Furey TS, Roskin KM, Sugnet CW, Haussler D, Kent WJ: The UCSC Table Browser data retrieval tool. *Nucleic Acids Res* 32: D493-496, 2004
  9. Huang da W, Sherman BT, Tan Q, Kir J, Liu D, Bryant D, Guo Y, Stephens R, Baseler MW, Lane HC, Lempicki RA: DAVID Bioinformatics Resources: expanded annotation database and novel algorithms to better extract biology from large gene lists. *Nucleic Acids Res* 35: W169-175, 2007
  10. Tomizuka K, Horikoshi K, Kitada R, Sugawara Y, Iba Y, Kojima A, Yoshitome A, Yamawaki K, Amagai M, Inoue A, Oshima T, Kakitani M: R-spondin1 plays an essential role in ovarian development through positively regulating Wnt-4 signaling. *Hum Mol Genet* 17: 1278-1291, 2008
  11. Yoshikawa M, Hishikawa K, Marumo T, Fujita T: Inhibition of histone deacetylase activity suppresses epithelial-to-mesenchymal transition induced by TGF-beta1 in human renal epithelial cells. *J Am Soc Nephrol* 18: 58-65, 2007

## FIGURE LEGENDS

**Supplemental Figure 1.** Characterization of PT-DMRs identified by D-REAM.

(A) 6387 PT-DMRs hypomethylated relative to the reference tissues, kidney, liver, and cerebrum, were classified as DMRs unique to a tissue or common to comparisons with at least two tissues.

(B) 5647 PT-DMRs hypermethylated relative to the reference tissues were classified in the same manner as in (A).

**Supplemental Figure 2.** Validation of the sorted kidney cells obtained from 10 week-old *db/db* mice.

Expressions of the marker genes of proximal tubules (*Sglt2* and *Pck1*), thick ascending loop of Henle (*NKCC2*), distal tubules (*NCC*) and collecting duct ( $\beta$ ENaC) in the PT and non-PT fractions (n = 4-5 per group; \*p < 0.05). In this and all other supplemental figures, error bars represent mean  $\pm$  SEM.

**Supplemental Figure 3.** Aberrant DNA methylation induced by diabetes in the PT cells.

(A) DNA methylation status of the target genes in the PT fraction obtained from 8-10 week-old *db/m* and *db/db* mice is shown (n = 5-9 per group; \*p < 0.05).

(B) Expression levels of the genes described in (A) are shown. *Cldn 18* mRNA was not



detected (n = 5 per group; \*p < 0.05).

**Supplemental Figure 4.** Blood glucose levels and body weight of 5- and 8-week old *db/m* and *db/db* mice (n = 13 per group; \*p < 0.05).

**Supplemental Figure 5.** Differential effects of pioglitazone on *db/db* mice.

(A, B) Urinary albumin excretion in 24 hours (A) and the plasma levels of triglyceride and non-esterified fatty acid (NEFA) (B) were determined at the end of 3 weeks' administration of pioglitazone to *db/db* mice (n = 6 per group; \*p < 0.05).

(C) *Acaca* mRNA expression with and without pioglitazone treatment in the PT cells. The mRNA levels in the PT cells obtained from *db/m* and *db/db* mice after 3 weeks' administration of pioglitazone or normal chow were quantified by quantitative RT-PCR (n=5 per group; \*p < 0.05).

(D) DNA methylation status of *Cldn18* with and without pioglitazone treatment. PT cells were collected from *db/m* and *db/db* mice after 3-weeks' administration of pioglitazone or normal chow. DNA methylation of *Cldn18* was analyzed by COBRA (n=5 per group; \*p < 0.05). The CpG site of *Cldn18* is indicated in Table 1. n.s. denotes not significant.

**Supplemental Figure 6.** Persistent histone modifications resistant to antidiabetic therapy with pioglitazone.

Histone H3K9 acetylation (A) and H3K4 tri-methylation (B) of the promoters of *Agt*,

*Abcc4*, and *Slc1a1* in the kidneys of *db/m* and *db/db* mice after 3-weeks'

administration of pioglitazone or normal chow (n = 4-8 per group; \*p < 0.05 vs control

mice). n.s. denotes not significant.

**Supplemental Table 1.** Tissue specificity of transcripts from genes associated with hypo-DMRs in the PT cells.

Comparison	Term	Count	P value
Kidney (1336/1935)	Embryo	206	$2.02 \times 10^{-10}$
	Mammary tumor	242	$1.94 \times 10^{-8}$
	Brain	563	$1.71 \times 10^{-7}$
	Thymus	223	$3.51 \times 10^{-7}$
	Eye	139	$1.72 \times 10^{-5}$
	Hippocampus	103	$3.64 \times 10^{-5}$
	Kidney	186	$6.07 \times 10^{-5}$
Liver (1148/1643)	Mammary tumor	226	$2.77 \times 10^{-11}$
	Kidney	173	$1.05 \times 10^{-6}$
	Embryo	161	$8.66 \times 10^{-6}$
	Bone marrow	118	$1.22 \times 10^{-5}$
	Mammary gland	161	$4.13 \times 10^{-5}$
Cerebrum (1491/2037)	Kidney	247	$3.17 \times 10^{-13}$
	Liver	327	$9.66 \times 10^{-8}$
Common (1057/1455)	Kidney	165	$6.62 \times 10^{-9}$
	Liver	220	$7.58 \times 10^{-6}$
	Spleen	78	$7.34 \times 10^{-5}$

Refseq transcripts harboring PT-DMRs between 6.0 kb upstream and 2.5kb downstream from their TSS were analyzed using the DAVID web server (<http://niaid.abcc.ncifcrf.gov>) for their tissue specificity of expression. Significantly (P-value less than  $1.0 \times 10^{-4}$ ) enriched terms in the "Uniprot tissue" (UP\_TISSUE), which are classified based on literature mining and reports for each gene, are indicated. PT-DMRs hypomethylated relative to the each reference tissue, namely the kidney, liver,

and cerebrum, and common to comparisons with at least two tissues are separately demonstrated. The numbers of DAVID IDs and their corresponding Refseq IDs associated with the PT-DMRs are indicated within parentheses in the left column. Counts indicate the number of genes involved in the term.

**Supplemental Table 2.** Tissue specificity of transcripts from genes associated with hyper-DMRs in the PT cells.

Comparison	Term	Count	P value
Kidney (1565/2128)	Forelimb	23	$2.59 \times 10^{-4}$
Liver (1202/1604)	Liver	326	$2.34 \times 10^{-26}$
	Plasma	25	$6.58 \times 10^{-11}$
	Kidney	159	$8.63 \times 10^{-5}$
Cerebrum (1342/1921)	Brain	582	$4.78 \times 10^{-10}$
	Eye	155	$7.60 \times 10^{-9}$
	Mammary tumor	240	$5.96 \times 10^{-8}$
	Cerebellum	154	$3.45 \times 10^{-7}$
	Hippocampus	111	$6.44 \times 10^{-7}$
	Brain cortex	72	$1.39 \times 10^{-6}$
	Embryo	187	$2.22 \times 10^{-6}$
Common (482/685)	brain	205	$6.15 \times 10^{-4}$

Tissue specificity of expression from the Refseq genes was analyzed in the same way as that for the analysis shown in Supplemental Table 1. There was no term with a P value of less than  $1.0 \times 10^{-4}$  in the genes associated with PT-DMRs hypermethylated relative to the whole kidney and common to two tissues.

**Supplemental Table 3.** Functions of genes associated with hypomethylated PT-DMRs.

Enrichment Score	Category	Term	Count	P value
7.77	GOTERM_CC_FAT	GO:0005739~mitochondrion	111	7.13 x 10 <sup>-17</sup>
	SP_PIR_KEYWORDS	mitochondrion	71	5.16 x 10 <sup>-13</sup>
	GOTERM_CC_FAT	GO:0044429~mitochondrial part	53	7.84 x 10 <sup>-11</sup>
	GOTERM_CC_FAT	GO:0019866~organelle inner membrane	34	5.90 x 10 <sup>-8</sup>
	GOTERM_CC_FAT	GO:0031966~mitochondrial membrane	37	1.08 x 10 <sup>-7</sup>
	GOTERM_CC_FAT	GO:0005743~mitochondrial inner membrane	32	1.89 x 10 <sup>-7</sup>
	GOTERM_CC_FAT	GO:0005740~mitochondrial envelope	37	4.85 x 10 <sup>-7</sup>
	GOTERM_CC_FAT	GO:0031967~organelle envelope	44	1.90 x 10 <sup>-6</sup>
	GOTERM_CC_FAT	GO:0031975~envelope	44	2.18 x 10 <sup>-6</sup>
	SP_PIR_KEYWORDS	mitochondrion inner membrane	19	7.26 x 10 <sup>-5</sup>
	GOTERM_CC_FAT	GO:0031090~organelle membrane	53	7.30 x 10 <sup>-5</sup>
5.28	SP_PIR_KEYWORDS	transit peptide	39	6.65 x 10 <sup>-7</sup>
	GOTERM_CC_FAT	GO:0005759~mitochondrial matrix	20	9.99 x 10 <sup>-6</sup>
	GOTERM_CC_FAT	GO:0031980~mitochondrial lumen	20	9.99 x 10 <sup>-6</sup>
	UP_SEQ_FEATURE	transit peptide:Mitochondrion	38	1.14 x 10 <sup>-5</sup>
4.18	SP_PIR_KEYWORDS	ribonucleoprotein	26	6.89 x 10 <sup>-6</sup>
	KEGG_PATHWAY	mmu03010:Ribosome	15	8.81 x 10 <sup>-6</sup>
	SP_PIR_KEYWORDS	ribosome	8	8.98 x 10 <sup>-6</sup>
	GOTERM_BP_FAT	GO:0006412~translation	28	1.08 x 10 <sup>-5</sup>
	SP_PIR_KEYWORDS	ribosomal protein	20	1.36 x 10 <sup>-5</sup>
	GOTERM_MF_FAT	GO:0003735~structural constituent of ribosome	18	1.53 x 10 <sup>-5</sup>
	GOTERM_CC_FAT	GO:0005840~ribosome	20	9.84 x 10 <sup>-5</sup>
	SP_PIR_KEYWORDS	protein biosynthesis	16	1.01 x 10 <sup>-4</sup>
	GOTERM_CC_FAT	GO:0033279~ribosomal subunit	10	7.08 x 10 <sup>-4</sup>
	GOTERM_MF_FAT	GO:0005198~structural molecule activity	28	0.00318
	GOTERM_CC_FAT	GO:0030529~ribonucleoprotein complex	30	0.00413
2.96	GOTERM_CC_FAT	GO:0005903~brush border	12	3.11 x 10 <sup>-8</sup>
	GOTERM_CC_FAT	GO:0031526~brush border membrane	5	0.00140
	GOTERM_CC_FAT	GO:0031253~cell projection membrane	5	0.0746
	GOTERM_CC_FAT	GO:0044463~cell projection part	8	0.446

The functions of the Kidney genes, that were revealed to be associated with hypomethylated PT-DMRs in Supplemental Table 1, were analyzed using the Functional Annotation Clustering tool provides by the DAVID web server. The category column indicates the annotation categories involving terms indicated in the term column. The table shows the clusters having terms for which the lowest P values were less than  $1.0 \times 10^{-4}$ .

**Supplemental Table 4.** Functions of genes associated with hypermethylated PT-DMRs.

Enrichment Score	Category	Term	Count	P value
2.60	GOTERM_CC_FAT	GO:0005739~mitochondrion	28	$5.87 \times 10^{-5}$
	SP_PIR_KEYWORDS	mitochondrion	19	$1.75 \times 10^{-4}$
	GOTERM_CC_FAT	GO:0005743~mitochondrial inner membrane	11	$4.24 \times 10^{-4}$
	GOTERM_CC_FAT	GO:0031966~mitochondrial membrane	12	$6.13 \times 10^{-4}$
	GOTERM_CC_FAT	GO:0019866~organelle inner membrane	11	$6.39 \times 10^{-4}$
	GOTERM_CC_FAT	GO:0005740~mitochondrial envelope	12	$1.01 \times 10^{-3}$
	SP_PIR_KEYWORDS	transit peptide	12	$2.18 \times 10^{-3}$
	GOTERM_CC_FAT	GO:0044429~mitochondrial part	13	$3.38 \times 10^{-3}$
	GOTERM_CC_FAT	GO:0031967~organelle envelope	12	$1.15 \times 10^{-2}$
	GOTERM_CC_FAT	GO:0031975~envelope	12	$1.18 \times 10^{-2}$
	UP_SEQ_FEATURE	transit peptide:Mitochondrion	10	$2.85 \times 10^{-2}$
	GOTERM_CC_FAT	GO:0031090~organelle membrane	14	$3.67 \times 10^{-2}$
	SP_PIR_KEYWORDS	mitochondrion inner membrane	5	$7.53 \times 10^{-2}$

The functions of genes with PT-DMRs hypermethylated relative to the liver, which were classified into Kidney expression, were analyzed in the same manner as that for the analysis shown in Supplemental Table 3.



**Supplemental Table 5.** Oligonucleotides used for the bisulfite PCR, and real-time PCR for cDNA and ChIP

Primers used for bisulfite PCR, sequencing

Name	Position (mm9)	F/R	Primer sequence (5' to 3')
Agt promoter A	chr8:127093342-127093686	F	TTGGTGATTTATAGGGGATAGTTTATT
		R	CAACCTCTATACAAAATAACCCAAAA
Agt promoter B	chr8:127093899-127094370	F	AGTTATGTAGATTTTGGGATGAAAGTT
		R	CCACCCATAATAACCTACAAATAAAAC

Primers used for bisulfite PCR, COBRA (mouse)

COBRA Name	Position (mm9)	Primer name	Primer sequence (5' to 3')
Abcb1b_bis	chr5:8799047-8799399	Abcb1b_db_bis_L	GTTTTATGTTGTTTGGGTGTTTATT
		Abcb1b_db_bis_R	AATTTACTTTCACCTTATACTTTCC
Abcc4_bis3	chr14:119102417-119102771	Abcc4_bis3_L	AAAGGGAAGAGAGGATATTAAGA
		Abcc4_bis3_R	CAACCAAATAATAACAACCCATACAA
Abcc4_bis2 <sup>a</sup>	chr14:119104158-119104491	Abcc4_db_bis2_L	AAGTTTTTTAGGTTTTTATATTTTA
		Abcc4_db_bis2_R	TTTCTACCTTTAATAACCATATCCC
Acsm2_bis1	chr7:126703699-126704056	Acsm2_bis1_L	CTATCTCTATTTATTCTTTCTCA
		Acsm2_bis1_R	GTGTGTATTTAGAGGATATATGATT
Acsm3_bis	chr7:126905846-126906210	Acsm3_bis_L	TAGGGGAGGAATAATAAATAGTGAAT
		Acsm3_bis_R	AAAAAATAAACAAAAAAAAACAAAAC
Acsm5_bis	chr7:126669794-126670111	Acsm5_bis_L	TTAATTTTGTTTTTTTTAGGTTGTGT
		Acsm5_bis_R	TTTCTTAACTCTTCCCTTCTTAAT

Acsm5_bis2	chr7:126669569-126669812	Acsm5_bis2_L	AGGTGAAAAATAGATAGGATTTGGT
		Acsm5_bis2_R	CTAAAAAAAACAAAATTAATAATCAAC
Agt_bis*	chr8:127093023-127093304	Agt_bis_F	GAATTTTAGAATTGTGATGAAGTTTGT
		Agt_bis_R	AATAACCAAATCCTTTTACCTCCTATA
Apob_bis1	chr12:7984976-7985261	Apob_bis_1L	TTGGAAAATATAAGAAAGTTAAGGT
		Apob_bis_1R	ACAATACACAAAAAACAAAAATCC
Cdc6_bis	chr11:98769822-98770210	Cdc6_db_bis_L	ATAAAAAACACAACATAATTAATAA
		Cdc6_db_bis_R	TAGTATTAAGGTAGGAAAGGTTGAG
Cldn10_bis2	chr14:119251094-119251362	Cldn10_bis2_L	TTAGTTTTTGTTTTTTGGAGTTGAGG
		Cldn10_bis2_R	AATTATTTCTTATTCTCTCTCTAAA
Cldn18_bis2	chr9:99610320-99610507	Cldn18_bis2_L	TAAGGAAAATAGTATGAGTAAATAT
		Cldn18_bis2_R	CAAAAAAACAAAAAACCCCTACCAC
Cldn18_bis <sup>a</sup>	chr9:99608935-99609176	Cldn18_db_bis_L	AGTAGGATAGGATTAAGATTATGTA
		Cldn18_db_bis_R	AATCAAAAAAACCATACAAAACC
Cpe_bis	chr8:67176010-67176379	Cpe_bis_L	GAAAATTAGAAGAGAGGTAAAATTA
		Cpe_bis_R	AACCCAAAAATTATTTTATAAACAC
Cpt1a_bis2	chr19:3321141-3321590	Cpt1a_bis2_L	TTCCTCCAACCTATTTTTATTTT
		Cpt1a_bis2_R	ATAGTTTTTTTTTTAAGGATTGTAGTTTT
Cpt2_bis2	chr4:107594088-107594385	Cpt2_bis2_F	GGTTGTGAGTTTAAGGTTTGTTTTAT
		Cpt2_bis2_R	CCTCAAATTAAACTCCTTACCAAAT
Cyp4a10_bis <sup>a</sup>	chr4:115191836-115192187	Cyp4a10_bis_L	AAAGGGAATTGGGAAGGGATAGTAT
		Cyp4a10_bis_R	CTAAAAACAAAAATAAACAAACAC

Cyp4a14_bis	chr4:115169988-115170321	Cyp4a14_bis_L	AACAAAAATCTCTAAAAAACCAACC
		Cyp4a14_bis_R	TAGGGAAGGAGAAAGGGTATAAAAT
Cyp4b1_bis1	chr4:115319229-115319486	Cyp4b1_bis1_L	TTAACAAAAACCCAACCAAAACC
		Cyp4b1_bis1_R	GGGAGAAATTATATTTTTAAAGTTTG
Cdc6_bis	chr11:98769822-98770210	Cdc6_db_bis_L	ATAAAAAACACAACCTAAATATTAATA
		Cdc6_db_bis_R	TAGTATTAAGGTAGGAAAGGTTGAG
Dmdgh_bis	chr13:94444987-94445328	Dmdgh_bis_L	TAAAAAAAAGAAAATTGTTAGGG
		Dmdgh_bis_R	TTACAACCTCAAAAACCTATTCTTAC
Enpep_bis	chr3:129035201-129035486	Enpep_bis_L	AATCCTAAAAAACAATAACT
		Enpep_bis_R	TTTAATTGAAAAGGGAAGTTAGTTG
Fbp2_bis2	chr13:62959666-62959958	Fbp2_bis2_L	TAAATCCCAAAACCTCCCTTACT
		Fbp2_bis2_R	AGGATTAATAAAATAAAATTGGGT
Fmo5_bis	chr3:97428284-97428659	Fmo5_bis_L	GGTTAGTAAATGGTTTTTTGATTG
		Fmo5_bis_R	TTTTATTTTATTCTTCTTTCCAC
G6pc_bis	chr11:101228839-101229131	G6pc_bis_L	GGTTGTTTTTGTTGTTTGTGTTTGT
		G6pc_bis_R	AATATTCATTCCTTCTCCATCCTT
G6pc_bis1 <sup>a</sup>	chr11:101229547-101229762	G6pc_bis1_L	CCTTACTCTAATTTATTTAACTTT
		G6pc_bis1_R	ATATAGTTTTATGGGGGAGTTTTTGT
Gclm_bis	chr3:121947769-121948149	Gclm_bis_L	TATTTGATTGGTTTGTAAAAAGT
		Gclm_bis_R	TTTCCTTTTACTTTACTTTACCCA
Gcnt1_bis <sup>a</sup>	chr19:17447400-17447702	Gcnt1_bis_L	TTGGATTAGGGGATTGAGGAAAATATA
		Gcnt1_bis_R	TCCCAAAAACCAAAATCTTTCAAA

Gent1_bis3	chr19:17434701-17435083	Gent1_bis3_L	TTTATTTTTTATTATTTTAGGTGAG
		Gent1_bis3_R	ATCTTCACCACCTTCCAAAAAACA
Gnmt_bis3	chr17:46863734-46864220	Gnmt_bis3_F	AATTGGGGTAAGTTTGTGTGTTAG
		Gnmt_bis3_R	TCCCAAAAACACATAAAACTCATT
Gstz1_bis	chr12:88489384-88489779	Gstz1_bis2_F	TTTAAGTTATTGTTGGAATGGAGTTG
		Gstz1_bis2_R	AAACACTAACAACAAACCACCTAAC
Gys1_bis	chr7:52690664-52691041	Gys1_bis_L	ATTTTTGTGTTTTGTGAAGGGGTT
		Gys1_bis_R	CTTCCCACCTTATATCTAAAAATT
Hadh_bis	chr5:30483161-30483590	Hadh_bis_L	AAAAATAAGAAATTATGTGAAAGAAA
		Hadh_bis_R	AACAAACTCCAAATACAAATCAAACC
Hist2h2aa2_bis	chr3:96048010-96048335	Hist2h2aa2_bis_L	GTAATTTTATTTGTTTTAGTTAAAG
		Hist2h2aa2_bis_R	ATACTCTTCTCTCATCCCTACAAATTA
Hnf4a_bis7 <sup>a</sup>	chr2:163373462-163373761	Hnf4a_bis7_F	AAAAATCAATCCTATCCAACATAACC
		Hnf4a_bis7_R	TGAAGTTGGGATATAAATTTAAAAAGG
Hnf4a_bis8	chr2:163373942-163374299	Hnf4a_bis8_F	TTTGTTTGGTGGTTTTGTATGGTA
		Hnf4a_bis8_R	AACCAACTCAAAAACACATATACCC
Kif20b_bis <sup>a</sup>	chr19:34995021-34995357	Kif20b_bis_L	TTACAAAACCAACACATACAAATAC
		Kif20b_bis_R	AGAAGGAAAAATGAAGAAAGAAATG
Ldhb_bis	chr6:142455910-142456212	Ldhb_bis_L	AGATTTTTTAATTTTTATAGGGATTT
		Ldhb_bis_R	CCCCTACCTATTTCTTCTTTATAATT
Lxr_bis1	chr2:91033432-91033826	Lxr_bis1_F	TTAGGAAGAGATGTTTTGTGGTTG
		Lxr_bis1_R	CCACTACCCAATAATACATCAAAA

Met_bis <sup>a</sup>	chr6:17438380-17438731	Met_bis_L	TAGTTTTTTGTTTTTGGAAATTTTGG
		Met_bis_R	AACTTTCCTTCTTTTACTAACAATA
Met_bis1	chr6:17438379-17438727	Met_bis1_L	TTAGTTTTTTGTTTTTGGAAATTTTGG
		Met_bis1_R	TTCCCTTCTTTTACTAACAATACTT
Met_bis2	chr6:17441163-17441486	Met_bis2_L	CTTCCATTTCTCTCTTTAATTTCTAA
		Met_bis2_R	GGATATTTTTTGAAGGTTTTTTGTTA
Met_bis2n	chr6:17435477-17435701	Met_bis2n_L	GGTGATTTGGTTTTATTTGTTATGTG
		Met_bis2n_R	CATATAATTTCTACCTCCATCCATT
Mgea5_bis <sup>a</sup>	chr19:45828419-45828766	Mgea5_gb_bis_L	CTTAAACAAAACAAAACAAAAAACC
		Mgea5_gb_bis_R	GGATTGAAAATGAAATAGAATTGAG
Nudt19_bis	chr7:36342624-36342990	Nudt19_bis_L	AGGAAGGAGTTAAGTTTTGATTTAA
		Nudt19_bis_R	AAAATATAATTATAACCCTCTAACAC
Pck1_bis	chr2:172978395-172978680	Pck1_bis_L	AGTTTAATTATTATTTTTTTGGAGT
		Pck1_bis_R	CTACCTACCTTTCTTCCTTTTAAAAA
Pck1_bisn	chr2:172979616-172979782	Pck1_bisn_L	AAATAAATAAAACCAAACCCCAAACC
		Pck1_bisn_L	TAGGATTTGTAGAGAATATTTAAT
Pck1_bisn1 <sup>a</sup>	chr2:172978288-172978547	Pck1_bisn1_L	ACATCAACAACAACAACAATCAAAA
		Pck1_bisn1_R	AAATATTATATAGAAGGGAGGATAG
Pdk3_bis2	chrX:91078798-91079165	Pdk3_bis2_L	AATTAGAAAAAAAAAAGGTAAAAG
		Pdk3_bis2_R	CACCCAAAAAAAAATAAATAACAACC
Pdp1_bis	chr4:11892199-11892514	Pdp1_bis_L	ACCCCATCCATTCTTTATAATATACT
		Pdp1_bis_R	GTTTTTTTTTATTTTTGTAGATATTG

Proc_bis1	chr18:32297365-32297769	Proc_bis1_F	ATTGTAAGATTGTGAAGGATTGTGG
		Proc_bis1_R	CTAATATCCCCCAAACCAAATAAAC
Serpina1e_bis1	chr12:105194600-105194996	Serpina1e_bis1_F	TTTTTGGGAGTAGGGGTAATATAGG
		Serpina1e_bis1_R	ACACAAATCTCCCAAACCACTATAC
Slc2a5_bis1 <sup>a</sup>	chr4:149493621-149493821	Slc2a5_bis1_L	ATTATTTCTATACCCACCTCTCA
		Slc2a5_bis1_R	GTTTTTTTTTAGGAAAATTTTTTTG
Slc2a5_bis2	chr4:149493893-149494137	Slc2a5_bis2_L	AAGGGTGAAGGATAAGAAGAAAGA
		Slc2a5_bis2_R	CAAACAAACTAAATCCCCAAAAA
Slc5a2_bis1 <sup>a</sup>	chr7:135408837-135409185	Slc5a2_bis1_L	AGGAATATGTATGTTTTGTTGATTGTT
		Slc5a2_bis1_R	AACTAATCCCTAAATTCCCCTAAAA
Slc5a2_bis	chr7:135411459-135411821	Slc5a2_bis_L	CAAACCCTAAACTAAAACATTTAC
		Slc5a2_bis_R	GATATTTAAGAAGGTTAGAAGTTT
Slco1a_F <sup>a</sup>	chr6:141895647-141896048	Slco1a_F	TGTGTGTGTATGGATTTGTTTGTTT
		Slco1a_R	AACCACTCTTCCCAAATTACTCTAA
Socs2_bis	chr10:94880798-94881161	Socs2_db_bis_L	TTTTCTCTTAAATAATTCTATACAC
		Socs2_db_bis_R	ATTTTTGTATATTGTAGAGGTTTAA
Suclg2_bis	chr6:95666262-95666607	Suclg2_bis_L	AATTTATTTTTTTTCCCACCAAACC
		Suclg2_bis_R	GGGTGAATGTTTTTTTTTTTTTGTTAATAG

<sup>a</sup> Primers used in Table 1, Figures 1, 2 and 4, and Supplemental Figures 3 and 5D.

Primers used for bisulfite PCR, COBRA (human)

COBRA Name	Position (GRCh37/hg19)	Primer name	Primer sequence (5' to 3')
AGT_bis	chr1:230850702-230850705	AGT_bis_L	CCAGTGTAGCTGGGGAGACTGTAAAC
		AGT_bis_R	CACTGAAGGGACAGGAAGGAAGATCCT

Primers used for real-time PCR for cDNA

Name	Accession Number	F/R	Sequence (5' to 3')
Acaca	NM_133360	F	CTGGAGGACCCAACAACAAC
		R	GAGCAGTTCTGGGAGTTTCG
Cyp4a10	NM_010011	F	TCCCATCACCTCCTTTTCAC
		R	TGCACGACACAATTTCTGT
Cyp4a14	NM_007822	F	CTCGGGGAGCAATATACGAG
		R	CATTCAACAGGAGCAAACCA
$\beta$ ENaC	NM_011325	F	TCGGAACTTCACGCCTATCT
		R	CCGATGTCCAGGATCAACTT
G6pc	NM_008061	F	CGAGGAAAGAAAAAGCCAAC
		R	CCAGAATCCAACCACAAGA
Gcnt1	NM_010265	F	CTGGAACCCAATGAAACCTT
		R	CAACAGCCATGCTAAATGGA
Hnf4a	NM_008261	F	AGAGGTTCTGTCCCAGCAGA
		R	ATGTACTTGGCCCACTCGAC
Kif20b	NM_183046	F	TTTCCTTAGTCGCCTCAAAC
		R	ATCCAAAACCTTGCACACAGC

Met	NM_008591	F	AGCATTTTTACGGACCCAAC
		R	ACAGCCGGAAGAGTTTCTCA
Mgea5	NM_023799	F	TACCAAGCCAAATGGTGACA
		R	ACACCTCCTGCTCTTCATGG
NCC	NM_001205311	F	CCTCCATCACCAACTCACCT
		R	CCGCCCACTTGCTGTAGTAT
NKCC2	NM_183354	F	TGTGAAGTTTGGATGGGTGA
		R	CAGGAGAGGCGAATGAAGAG
Pck1	NM_011044	F	AGGAGTACGGGCAGTTGCT
		R	TCTGCTCTTGGGTGATGATG
Sglt2	NM_133254	F	CTGAACTTGGGGAGCAGAAG
		R	GGCAGCGATAACCAGAATGT
Slc2a5	NM_019741	F	TACAACGTAGCTGCCGTCAA
		R	CAGCGTCAAGGTGAAGGACT
Slc1a1	NM_013797	F	TTAAAGCCAACGCAAGATCC
		R	GGGAGTTTCACCAATTCCAC

Primers used for real-time PCR for ChIP (mouse)

Name	Position (mm9)	F/R	Sequence (5' to 3')
Agt	chr8:127093635-127093725	F	TACTCAAGGGGTGGAGATGG
		R	AGCCTGGATTCTCATGGTTC

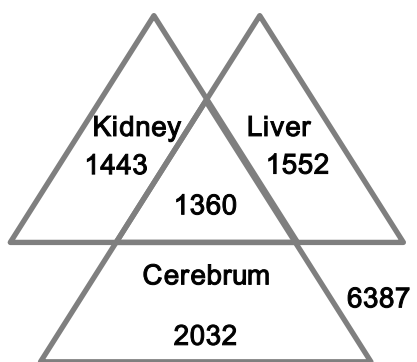


Abcc4	chr14:119105134-119105270	F	GTGTAAGGCTGTGCAGGAAA
		R	GCGTGTTCTTCTGGTGAGTG
Slco1a1	chr6:141895639-141895725	F	CAACAGAAGGCCACTCTTCC
		R	TGAACCACCACCTCCCTATC

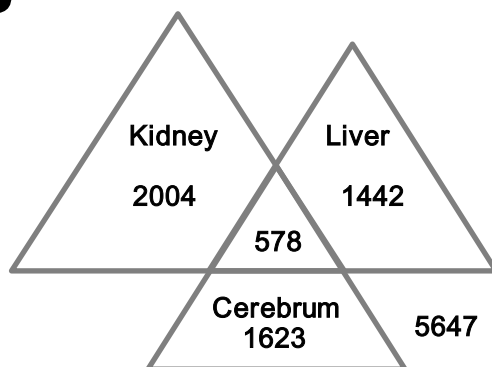
Primers used for real-time PCR for ChIP (human)

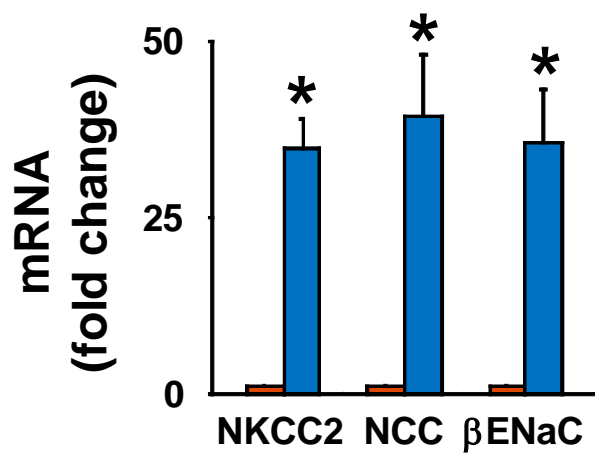
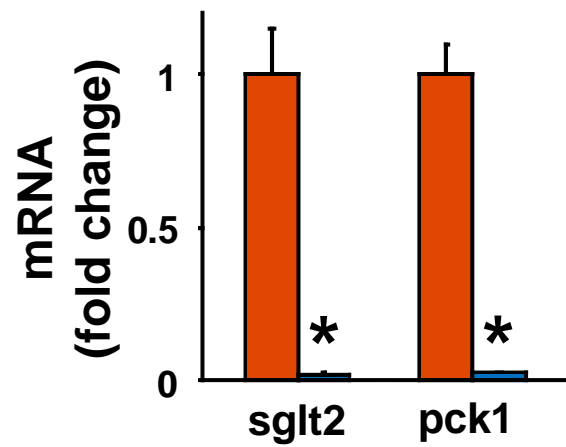
Name	Position (GRCh37/hg19)	F/R	Sequence (5' to 3')
AGT	chr1:230850646-230850747	F	AACAGGGCATGACAGAGACC
		R	TAAGGCTGGACACATCACCA

**A**

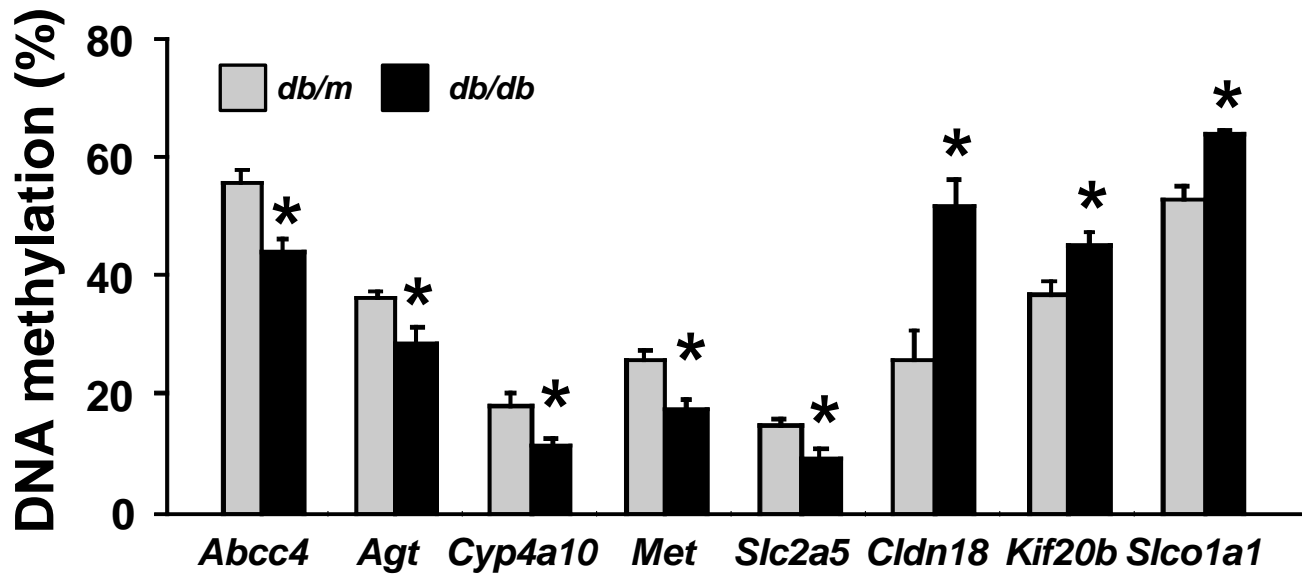
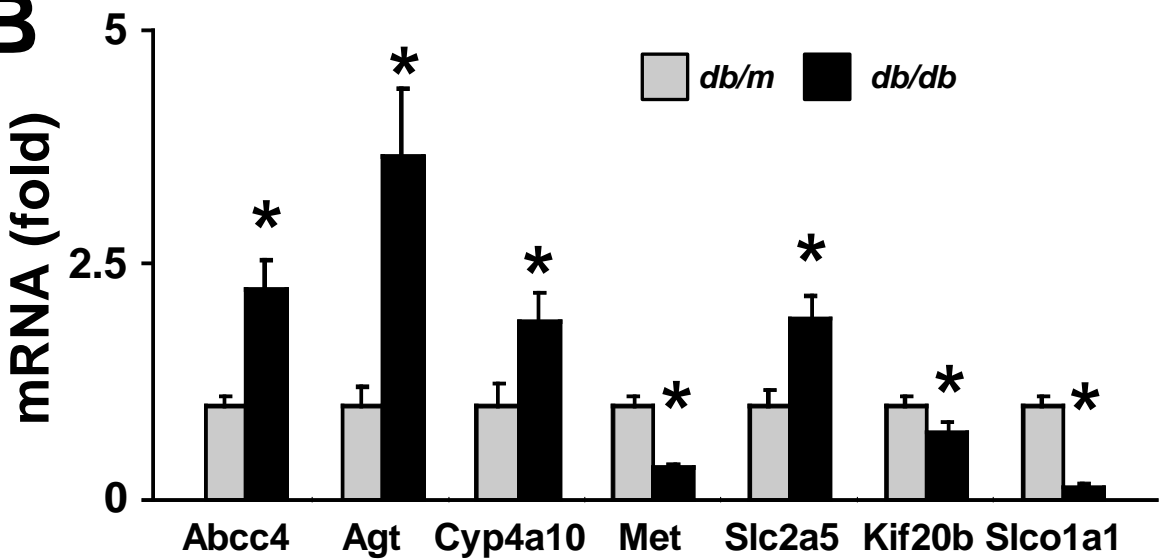


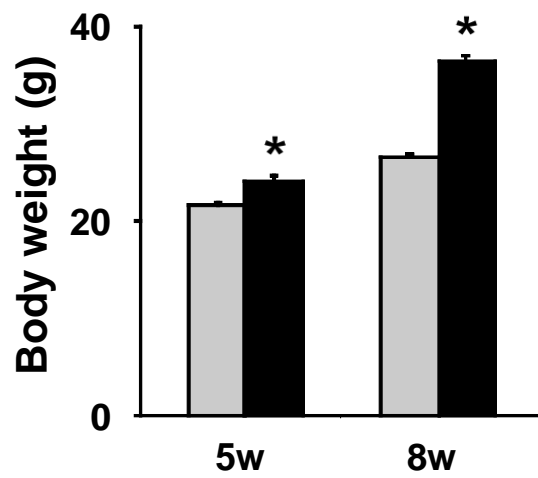
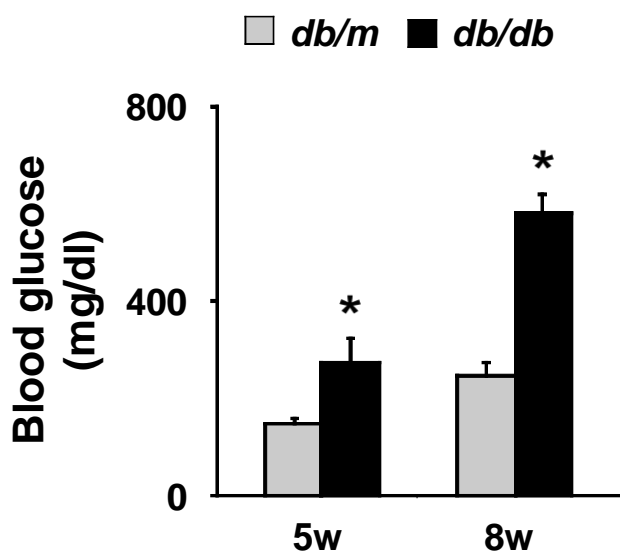
**B**



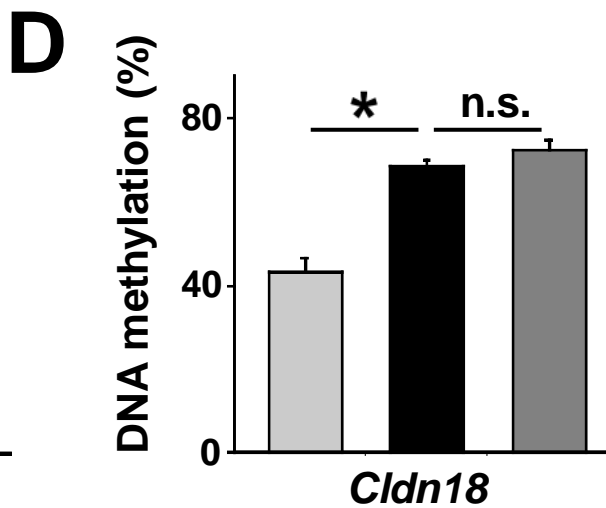
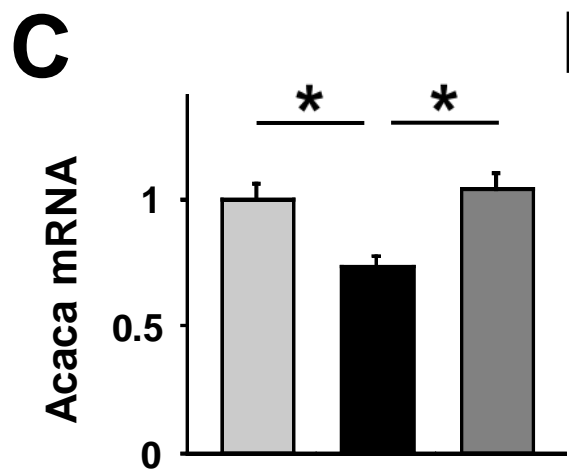
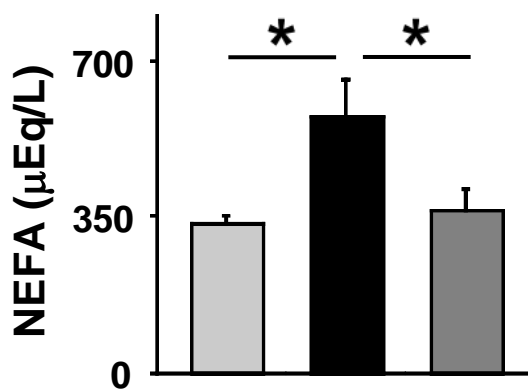
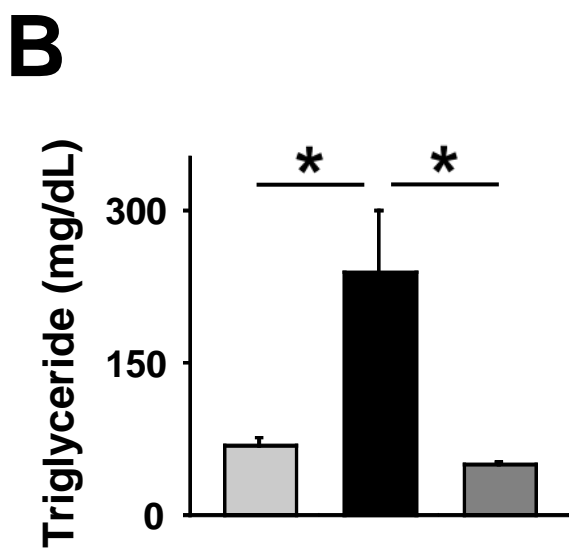
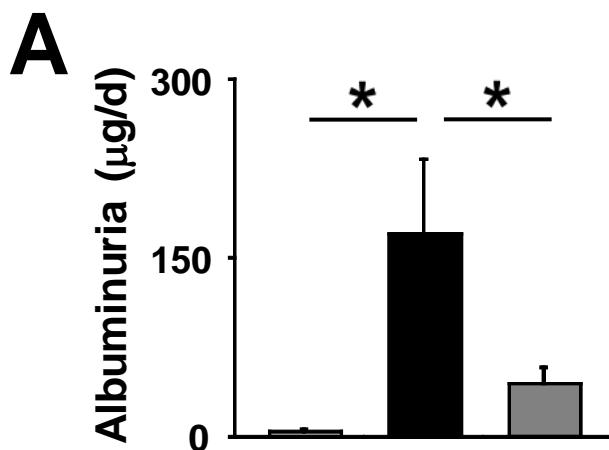


Supplemental Figure 2

**A****B**



Supplemental Figure 4

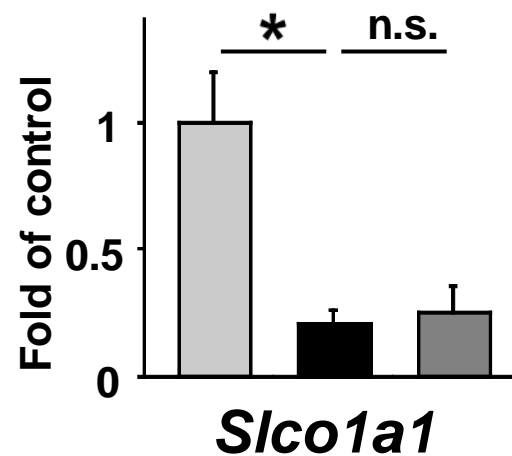
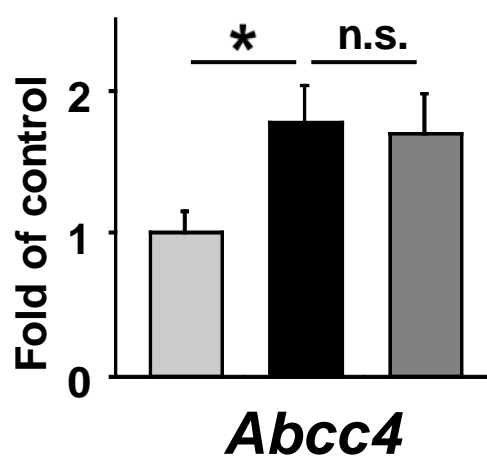
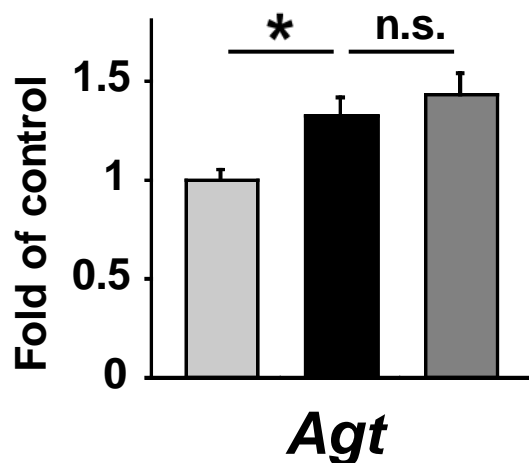


Supplemental Figure 5

db/m db/db db/db piog

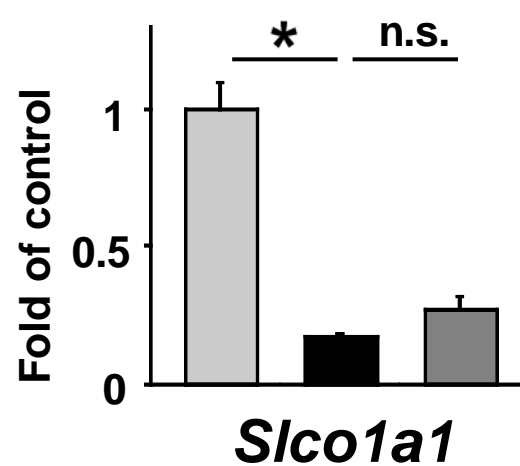
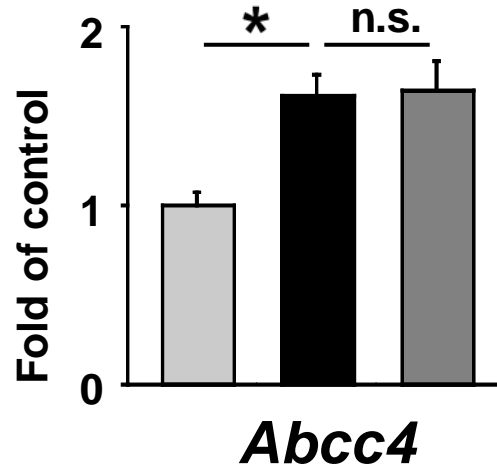
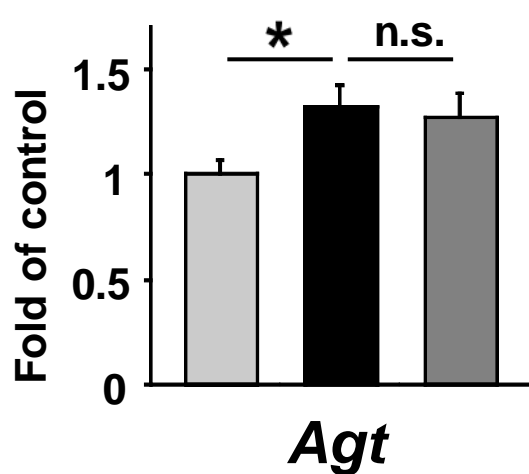
**A**

**H3K9Ac**



**B**

**H3K4me3**



Supplemental Figure 6